THE FAR-INFRARED SPECTRUM OF HYDROGENATED AMORPHOUS CARBON AND THE 21, 27, AND 33 MICRON FEATURES IN CARBON-RICH PROTO–PLANETARY NEBULAE

V. I. GRISHKO,[1] K. TERESZCHUK,[2] W. W. DULEY,[1] AND P. BERNATH[1,2]

ABSTRACT

We report laboratory emission spectra of hydrogenated amorphous carbon (HAC) in the wavelength range 19 μm $< \lambda <$ 120 μm (525–83 cm^{-1}) at temperatures between 300°C and 500°C. These spectra show emission features at 21, 27, and $\approx$33 μm (475, 370, and 303 cm^{-1}) that can be identified with similar bands in the far-infrared spectra of extreme carbon stars, proto–planetary nebulae, and planetary nebulae. It is suggested that HAC is present in these objects but that the chemical composition of this material depends on the evolutionary state. We also detect a number of broad features at wavelengths longer than 40 μm, attributable to chemical groups in HAC. A strong feature is observed at $\approx$60 μm (165 cm^{-1}) in laboratory spectra and may be present in spectra of the carbon-rich planetary nebula CPD −56°8032. We briefly discuss the nature of the chemical groups responsible for the appearance of these features.

Subject headings: circumstellar matter — infrared: ISM — infrared: stars — ISM: lines and bands — ISM: molecules — stars: AGB and post-AGB

1. INTRODUCTION

Infrared emission spectroscopy of carbon-rich asymptotic giant branch (AGB) and post-AGB objects such as proto–planetary nebulae (PPNs) and planetary nebulae (PNs) has revealed a wealth of spectral features extending from 3.28 to 30 μm (see reviews by Tokunaga 1996, Geballe 1997, and Kwok, Volk, & Hrivnak 1999). These spectra consist of a variety of relatively narrow bands at 3.28, 3.4, 6.2, 7.7, 8.6, and 11.3 μm generally attributed to vibrational modes of aromatic hydrocarbon molecules (Duley & Williams 1981; Leger & Puget 1984; Allamandola, Tielens, & Barker 1985) superposed on broad plateau components possibly associated with larger carbonaceous particles containing up to 10^4 carbon atoms (Allamandola, Tielens, & Barker 1989). These larger particles have both aliphatic (Kwok, Volk, & Bernath 2001) and aromatic components. The mixed sp^2/sp^3 bonded composition of this material appears to be very similar to that existing in hydrogenated amorphous carbon (HAC) as indicated by comparison between emission and absorption spectra of HAC and interstellar sources (Ogmen & Duley 1988; Scott, Duley, & Jahani 1997; Chiar et al. 2000).

The extension of IR spectra to long wavelengths has resulted in the discovery of many other emission features in carbon-rich circumstellar shells, PPNs, and PN sources (see the summary by Kwok et al. 1999). Most notable are a series of broad bands at or near 20, 27, and 30 μm (Kwok, Volk, & Hrivnak 1989; Omont et al. 1995; Volk, Xiong, & Kwok 2000). There are indications of additional weaker features over this wavelength range as well as other broad bands at longer wavelengths (Volk et al. 2000). In addition, the relative strength of the 21, 27, and 30 μm features appears to depend on the evolutionary state of the emitting object (Kwok et al. 1999), with the 21 μm feature appearing strongly only in PPNs while the 30 μm band is present in extreme carbon stars, PPNs, and PNs.

There have been numerous suggestions as to the origin of these long-wavelength features (Buss et al. 1990; Webster 1995;

Hill, Jones, & d'Hendecourt 1998; Papoular 2000; von Helden et al. 2000), but all three main bands have yet to be firmly identified. The detection of these broad bands in carbon-rich objects, together with the fact that they are often found in sources also exhibiting the aromatic hydrocarbon features, implies that the carriers of the 21, 27, and 30 μm emission peaks could be associated with hydrocarbon material. IR spectra of individual molecules in this spectral range (Bentley, Smithson, & Rozek 1968) show that bending and skeletal deformation modes in a variety of hydrocarbon groups appear between 20 and 40 μm. The composition of HAC (Akkerman, Efstathiadis, & Smith 1996) includes alkene and cycloalkane groups with modes in this region, but spectra of HAC at wavelengths greater than 15 μm have not been available until now.

In this Letter, we report the first emission spectra of HAC in the range 19 μm $< \lambda <$ 120 μm. This extension of spectral data for HAC into the far-IR reveals a number of emission peaks characteristic of the hydrocarbon components of this material, including bands near 21, 27, and 33 μm. These data suggest that emission from HAC may contribute to the broad long-wavelength bands observed in the spectra of extreme carbon objects, PPNs, and PNs.

2. EXPERIMENTAL SYSTEM

Samples of the HAC material were deposited on a molybdenum substrate using laser ablation of graphite in the presence of hydrogen. The deposition chamber was continuously evacuated, maintaining a slow flow of pure hydrogen. The pressure was 0.7–1 torr. The ablation source was an XeCl excimer laser, operating at 308 nm with 70 mJ pulse^{-1}. Laser radiation was focused on the graphite target 4 cm from the molybdenum substrate. The products of laser ablation react with hydrogen to form HAC, which is deposited as an adherent layer on the surface of the substrate. At a pulse frequency of 10 Hz, a 1 μm thick HAC layer can be deposited in approximately 1 hr.

The molybdenum substrate was then placed in a mount inside a stainless steel chamber containing an emission port. The substrate was then subsequently heated to 300°C, 400°C, and 500°C, and thermal emission from the HAC/Mo sample was recorded using a Bruker IFS 120 HR Fourier transform spectrometer. The sample chamber and spectrometer were con-

[1] Department of Physics, University of Waterloo, 200 University Avenue West, Waterloo, ON N2L 3G1, Canada; wwduley@uwaterloo.ca.
[2] Department of Chemistry, University of Waterloo, Waterloo, ON N2L 3G1, Canada.
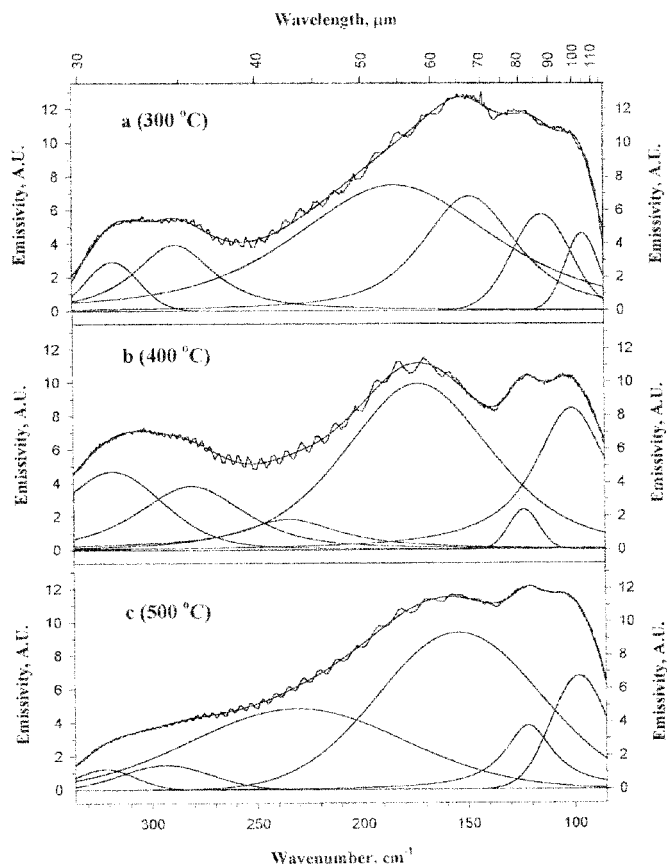
FIG. 1.—The 30–120 μm emission spectra of HAC at 300°C, 400°C, and 500°C. Spectral components (Table 1, in arbitrary units) are shown.

nected to the same vacuum system. No window was used between the sample chamber and spectrometer for measurements at $\lambda > 29$ μm, while a polyethylene window was used at shorter wavelengths. Spectra were recorded using a liquid He-cooled Si bolometer (30–120 μm) and an Si : B detector at 19–29 μm with a 3.5 μm Mylar beam splitter. The spectrometer was operated at 1 cm^{-1} resolution between 50 and 400 cm^{-1}, and 500 scans were co-added for the bare Mo reference and the HAC samples. Two hundred scans were averaged for the 19–29 μm spectra.

3. RESULTS

Emission spectra of HAC between 85 and 330 cm^{-1} (120–30 μm) recorded at 300°C, 400°C, and 500°C are shown in Figure 1. These emission spectra were obtained by ratioing HAC/Mo and Mo intensities at each temperature. This ratio was typically 1.3–1.4. The emissivity of Mo is featureless over this spectral region (Bramson 1968) and, at 500°C, decreases from 0.035 at 500 cm^{-1} (20 μm) to 0.015 at 100 cm^{-1} (100 μm). The baseline was assigned by assuming that the incremental emissivity of HAC/Mo versus Mo was zero at both ends of the measurable spectral range. Gaussian fit parameters to HAC spectra were obtained using the BOMEM GRAMS/386 v.3.04 software package with the assumption of a linear background and are listed in Table 1.

All spectra show an emission feature between 31 and 36 μm (322 and 278 cm^{-1}) and additional structure at longer wavelengths, but the relative strength of individual bands changes with sample temperature. This change is likely due to variations

TABLE 1
DECONVOLUTION OF SPECTRA FROM FIGURE 1

Wavelength (cm^{-1})	Wavelength (μm)	Peak Height (Arbitrary Units)	FWHM (cm^{-1})	Peak Area (% of Total)
300°C Temperature				
317	31.5	2.9	29	4.4
288	34.7	3.9	45	11.4
184	54.4	7.5	111	47.1
148	67.5	6.8	53	22.7
114	87.5	5.7	33	10.1
95	105	4.6	19	4.3
400°C Temperature				
318	31.5	4.7	57	11.8
281	35.6	3.8	60	13.5
235	42.6	1.8	58	7.1
173	57.8	9.9	82	46.2
123	81.0	2.4	17	2.2
101	99.2	8.5	42	19.2
500°C Temperature				
322	31	1.2	33	1.9
294	34	1.5	50	4.0
231	43	4.8	119	31.3
155	64.5	9.4	90	45.3
122	82	3.8	28	7.5
98	102	6.8	32	10.0

NOTE.—Peak area is shown in percentage of total area without any correction.

in the chemical composition of HAC on heating (Smith 1984; Scott & Duley 1996). At 300°C, spectral features occur at (31.5, 34.7) μm (317, 288 cm^{-1}), 54.4 μm (184 cm^{-1}), 67.5 μm (148 cm^{-1}), 87.5 μm (114 cm^{-1}), and 95.2 μm (105 cm^{-1}). The (31.5, 34.7) μm band is much weaker in spectra obtained at 500°C and is replaced by a single broad feature at 43.3 μm (231 cm^{-1}). These spectra also show narrow fringes that are artifacts; however, the amplitude of these fringes is small compared to all major Gaussian components and have been removed in determining the fits given in Tables 1 and 2.

Figure 2 shows the emission spectrum of HAC at 500°C in the region between 19 and 29 μm (525 and 345 cm^{-1}). A broad structured peak can be seen near 22 μm (455 cm^{-1}) together with a stronger, relatively narrow feature at 27 μm (370 cm^{-1}). The large overlap between the bands in the 22 μm feature makes the assignment of individual components somewhat ambiguous, but deconvolution of this emission into individual spectral peaks (Table 2) reveals a number of major components near 20.2, 21.6, and 23.6 μm (494, 463, and 424 cm^{-1}).

4. DISCUSSION

Spectral features appearing at or near 21, 27, and 33 μm in Figures 1 and 2 are consistent with the major long-wavelength

TABLE 2
DECONVOLUTION OF SPECTRA FROM FIGURE 2 AT 500°C

Wavelength (cm^{-1})	Wavelength (μm)	Peak Height (Arbitrary Units)	FWHM (cm^{-1})	Peak Area (% of Total)
513	19.5	0.27	8.9	2.5
494	20.2	0.35	26	9.8
479	20.9	0.145	7.7	1.2
463	21.6	0.54	44	25.4
424	23.6	0.67	31	21.8
402	24.9	0.41	17	7.6
371	27.0	1.44	21	31.7

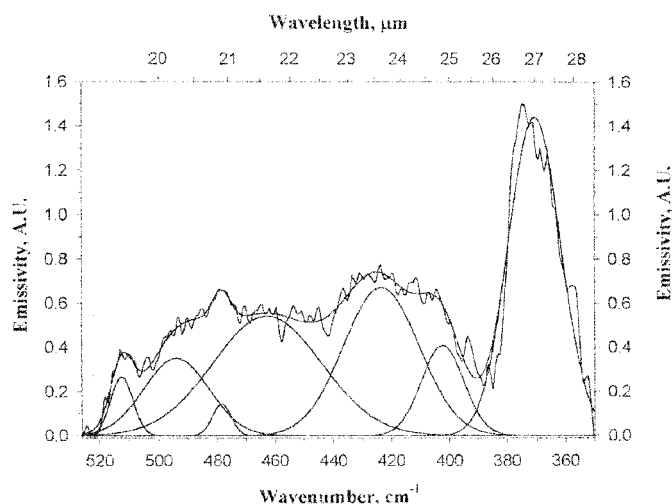NOTE.—Peak area is shown in percentage of total area without any correction.

FIG. 2.—Emission spectra of HAC between 19 and 29 μm recorded at 500°C. The component parameters are listed in Table 2.

bands observed in extreme carbon stars, carbon-rich PPNs, and PN sources (Kwok et al. 1999), suggesting that HAC is present in these objects. Indications of broad substructure in the laboratory emission bands implies that additional components could be present in the astronomical spectra. Our data also show a number of other peaks at $\lambda > 40$ μm that can be attributed to vibrational modes of chemical groups in HAC. In particular, the strong feature near 60 μm (165 cm^{-1}) can be identified with a band at the same wavelength observed in certain late WC-type PNs such as CPD $-56°8032$ (Cohen et al. 1999).

Most hydrocarbon molecules containing C$-$C and C$=$C bonds have skeletal deformation and torsional modes (Bentley et al. 1968) that can give rise to absorption at wavelengths in the 20–120 μm range. As chemical groups containing these bonds are the primary components of HAC, it is not surprising that HAC exhibits emission in this region. In addition, vibrational modes involving interlayer motion in aromatic clusters are predicted to occur at wavelengths longer than 80 μm (Seahra & Duley 2000). Specifically, the broad bands near 27 and 33 μm may arise from deformation modes in R$-$CH$-$CH$=$CH$-$CH$_3$ structures in alkenes (Bentley et al. 1968), where R is another hydrocarbon group. Torsional modes in C$=$CH$_3$ bonds have been found to produce bands in the 50–100 μm region in a variety of compounds, including those containing CH$_3$ groups attached to aromatic rings (Shimanouchi 1967; Bentley et al. 1968), while alkenes and cycloalkanes are both strong absorbers at 21 μm.

The changes in spectral distribution that occur with temperature (Fig. 1) can be attributed to different concentrations of sp^2- and sp^3-bonded carbon. Generally, HAC prepared at low temperature is characterized by an enhancement of the concentration of sp^3-bonded groups. These convert through loss of hydrogen to sp^2-bonded groups such as those found in alkenes and polycyclic aromatic hydrocarbon compounds (Akkerman et al. 1996). This process is complex and involves a number of intermediate species including nonaromatic ring structures. Emission and absorption bands due to these species can be seen in the 3.2–3.6 μm spectrum of HAC (Grishko & Duley 2000).

Similar changes in composition might be expected in the outflows from extreme carbon stars and in PPNs and PN sources where the 21, 27, and 33 μm bands have been observed (Volk et al. 2000). In such objects, the formation and subsequent evolution of these carriers should be strongly influenced by temperature and pressure conditions in the expanding shell as well as by the radiative environment where the dust is observed. Our spectra show that the hydrocarbon component responsible for emission in the 30–36 μm region is suppressed at high temperature (Fig. 1).

Deconvolution of the emission from 30 μm sources has demonstrated that the primary component of this band occurs at 33 μm (300 cm^{-1}) with FWHM = 95 cm^{-1}. Our spectra of 300°C material (Fig. 1) show a somewhat sharper feature with FWHM = 80 cm^{-1} peaking at approximately the same wavelength. We find that this band can also be resolved into two narrower components. At 400°C, this band is broader and less structured with an FWHM comparable to the interstellar feature. Additional features are seen in the emission spectrum of HAC at longer wavelengths (Fig. 1), including major components near 60 and 100 μm (165 and 100 cm^{-1}). There is some indication that such features may be present in extreme carbon stars such as IRAS 17534$-$3030 (Volk et al. 2000), but further observations and additional laboratory experiments are required to verify this identification.

5. CONCLUSIONS

Far-infrared emission spectra of HAC have been obtained and contain a number of broad components associated with low-energy vibrational resonances in a variety of hydrocarbon components. The major far-infrared bands observed near 21, 27, and 33 μm in various extreme carbon stars, PPNs, and PN sources are present in these spectra of HAC, suggesting that hydrogenated amorphous carbon may be a significant condensate in these carbon-rich objects. We observe changes in the relative intensity of these laboratory bands that may be useful in developing a connection between spectra and evolutionary status in these objects.

REFERENCES

Akkerman, Z. L., Efstathiadis, H., & Smith, F. W. 1996, J. Appl. Phys., 80, 3068
Allamandola, L. J., Tielens, A. G. G. M., & Barker, J. R. 1985, ApJ, 290, L25
———. 1989, ApJS, 71, 733
Bentley, F. F., Smithson, L. D., & Rozek, A. L. 1968, Infrared Spectra and Characteristic Frequencies 700–300 cm^{-1} (New York: Interscience)
Bramson, M. A. 1968, Infrared Radiation: A Handbook for Applications (New York: Plenum)
Buss, R. H., Jr., Cohen, M., Tielens, A. G. G. M., Werner, M. W., Bregman, J. D., Witteborn, F. C., Rank, D., & Sandford, S. A. 1990, ApJ, 365, L23

Chiar, J. E., et al. 2000, ApJ, 537, 749
Cohen, M., et al. 1999, ApJ, 513, L135
Duley, W. W., & Williams, D. A. 1981, MNRAS, 196, 269
Geballe, T. 1997, in ASP Conf. Ser. 122, From Stardust to Planetismals, ed. Y. J. Pendleton & A. G. G. M. Tielens (San Francisco: ASP), 119
Grishko, V. I., & Duley, W. W. 2000, ApJ, 543, L85
Hill, H. G. M., Jones, A. P., & d'Hendecourt, L. B. 1998, A&A, 336, L41
Kwok, S., Volk, K., & Bernath, P. 2001, ApJ, 554, L87
Kwok, S., Volk, K., & Hrivnak, B. J. 1989, ApJ, 345, L51
———. 1999, A&A, 350, L35

Leger, A., & Puget, J. L. 1984, A&A, 137, L5
Ogmen, M., & Duley, W. W. 1988, ApJ, 334, L117
Omont, A., et al. 1995, ApJ, 454, 819
Papoular, R. 2000, A&A, 362, L9
Scott, A., & Duley, W. W. 1996, ApJ, 472, L123
Scott, A., Duley, W. W., & Jahani, H. R. 1997, ApJ, 490, L175
Seahra, S. S., & Duley, W. W. 2000, ApJ, 542, 898

Shimanouchi, T. 1967, Natl. Stand. Ref. Data, 6, 1
Smith, F. W. 1984, J. Appl. Phys., 55, 764
Tokunaga, A. T. 1996, in ASP Conf. Ser. 124, Diffuse Infrared Radiation and
   the *IRTS*, ed. H. Okada, T. Matumoto, & T. L. Roellig (San Francisco: ASP),
   149
Volk, K., Xiong, G.-Z., & Kwok, S. 2000, ApJ, 530, 408
von Helden, G., et al. 2000, Science, 288, 313
Webster, A. 1995, MNRAS, 277, 1555